RSC Advances

PAPER

View Article Online
View Journal | View Issue

Cite this: *RSC Adv.*, 2020, **10**, 43383

Intra-mitochondrial reaction for cancer cell imaging and anti-cancer therapy by aggregation-induced emission†

Sangpil Kim,‡ Juhee Kim,‡ Batakrishna Jana and Ja-Hyoung Ryu *

Received 31st August 2020
Accepted 22nd November 2020

DOI: 10.1039/d0ra07471c

rsc.li/rsc-advances

Controlled intracellular chemical reactions to regulate cellular functions remain a challenge in biology mimetic systems. Herein, we developed an intra-mitochondrial bio-orthogonal reaction to induce aggregation induced emission. *In situ* carbonyl ligation inside mitochondria drives the molecules to form nano-aggregates with green fluorescence, which leads to depolarization of the mitochondrial membrane, generation of ROS, and subsequently mitochondrial dysfunction. This intra-mitochondrial carbonyl ligation shows great potential for anticancer treatment in various cancer cell lines.

Introduction

Intracellular reactions are essential for producing bioactive molecules that regulate cellular functions.[1,2] Intracellular reactions are genetically regulated and selectively catalyzed by enzymes, which convert specific reactants into distinct products for unique biological purposes.[3] For example, oxidation reactions such as in the citric acid cycle occur in the mitochondria, and the polymerization process of alpha–beta tubulin takes place in microtubules.[4] Thus, synthetic control of intracellular reactions has attracted much attention, as it may regulate subsequent cellular functions. Recently, extensive efforts have been made to design controlled chemical reactions in living cells; in particular, bio-orthogonal reactions that do not react with various cellular functional groups have been utilized for artificial chemical reactions. For example, Rao *et al.* developed an intracellular cyclization reaction for luciferin to form a nano-aggregation in tumor cells.[5–7] However, although synthetic intracellular reactions have been reported, the complex intracellular environment requires higher bio-orthogonality to improve specificity.[6]

Bio-orthogonal reactions, including click chemistry, Staudinger ligation, and *trans*-cyclooctene/tetrazine cycloaddition, are chemical reactions that occur without interference from biological materials in living systems.[8] Among these, carbonyl ligation reactions are of significant interest for their selectivity and unobstructed reactive groups that can react regardless of the presence of other functional groups.[9,10] These reactions have been used to pull down specific proteins, or to selectively modify functional proteins. The *in vitro* applicability of carbonyl ligation was also shown in labeling the surface of living cells.[11,12] As such unique reactions do not exist in the living cell, they may be controllable in the intracellular environment, and may be utilized to develop an artificial chemical system to control cellular fate.[13–15] Nevertheless, designing efficient bio-orthogonal reactions that can respond to driving processes in a dynamic intracellular environment, is still a challenge. It is also important that these reactions occur at a particular subcellular location to control specific cellular functions, as various signaling pathways are controlled by spatial separation of proteins inside the cell.[16,17] Thus, it is necessary to develop location-specific intracellular reactions for efficient applicability.

Mitochondria are important organelles that play a pivotal role in performing cellular functions such as ATP production, metabolic regulation, and programmed cell death. Specifically, targeting the mitochondria offers a promising strategy to activate cell death pathways.[18–20] Furthermore, the mitochondrial membranes of cancer cells are more negatively charged than those of normal cells; thus bioactive molecules may be accumulated in the mitochondria of cancer cells by conjugation with lipophilic cations such as triphenylphosphonium (TPP).[21] Recently, we reported that building blocks accumulate in the mitochondria following conjugation with the TPP moiety, leading to desirable conditions for synthetic chemical reactions inside mitochondria.[22–24] TPP-siloxane accumulated inside the mitochondria, and subsequent condensation reactions were confirmed. This reaction exacerbates dysfunction of mitochondria, suggesting that such synthetic reactions can be applicable for anticancer treatment. Based on these results, we hypothesized that targeting mitochondria would represent a novel strategy for promoting efficient bio-orthogonal reactions to regulate cellular function (Scheme 1).

Department of Chemistry, Ulsan National Institute of Science and Technology (UNIST), Ulsan 44919, Republic of Korea. E-mail: jhryu@unist.ac.kr

† Electronic supplementary information (ESI) available. See DOI: 10.1039/d0ra07471c

‡ These authors contributed equally to this work.

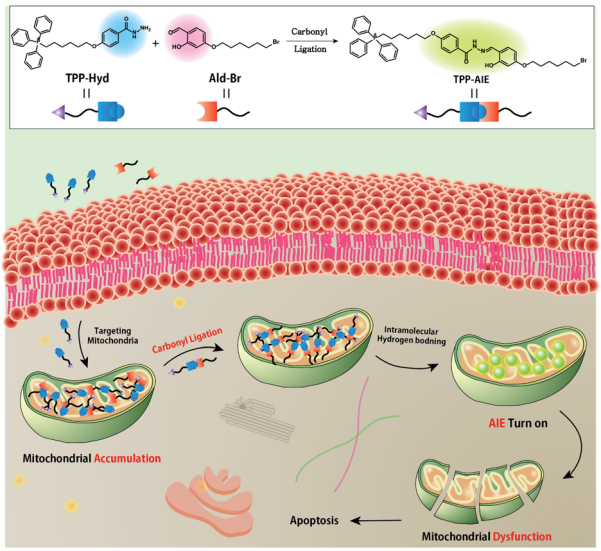

Scheme 1 Schematic illustration showing mitochondria targeting carbonyl ligation for formation of nanoparticle with AIE property.

Herein, we report a mitochondria-targeting carbonyl ligation system using a TPP-conjugated aldehyde. The accumulation of this reagent inside the mitochondria, in such a confined space, increases the concentration of this building block, which promotes conditions for effective carbonyl ligation. This reaction results in the formation of hydrazone, which contributes to the self-assembly of a nanostructure with aggregation-induced emission (AIE) properties *via* intramolecular hydrogen bonding. In addition, owing to the targeting ability of TPP, these reactions preferentially occurred in cancer cells rather than normal cells. The nanoparticles drive mitochondrial dysfunction, which leads to activation of apoptosis in these cancer cells. These results indicate that a mitochondria-targeting bio-orthogonal reaction represents a potential strategy to introduce an artificial intracellular chemical system that can regulate cellular functions.

Results and discussion

Carbonyl ligation using hydrazine

TPP-hydrazine (TPP-Hyd) and aldehyde-Br (Ald-Br) were synthesized from 2,4-dihydroxybenzaldehyde and purified by high-performance liquid chromatography (HPLC). To validate the effects of this bio-orthogonal reaction, a TPP-methoxy (TPP-Met) with a methoxy group instead of a hydrazine group was also synthesized as a control molecule. The hydrazine group of TPP-Hyd and the aldehyde group of Ald-Br react with each other to form TPP-AIE, which demonstrated increased intermolecular hydrogen bonding. In addition, TPP-AIE has a stronger fluorescence signature compared to TPP-Hyd or Ald-Br, due to the aggregation-induced emission properties caused by hindrance of molecular rotation.[18,25] The carbonyl ligation of TPP-Hyd with Ald-Br in a test tube was first confirmed by HPLC. On incubation of TPP-Hyd with Ald-Br for 24 h in pH 8.0 PBS (a solution mimicking the mitochondrial environment), the intensity of TPP-Hyd (T_R [retention time] = 3.2 min) and Ald-Br (T_R = 15.3 min) were decreased, and a new peak corresponding to TPP-AIE (T_R = 14.7 min) emerged, suggesting that carbonyl ligation can occur efficiently (Fig. 1a). In contrast, there was no appearance of a new peak in the reaction mixture of TPP-Met and Ald-Br (Fig. S1†). The reaction was further confirmed by fluorescence spectra at 365 nm excitation; TPP-Ald and Ald-Br did not show any fluorescence emission, but TPP-AIE, which possesses AIE properties through intermolecular hydrogen bonding, emitted green fluorescence (Fig. S2†).[26] Aggregation was further confirmed by Dynamic Light Scattering (DLS) with the mixture of 1 mM TPP-Hyd and Ald-Br in pH 8.0 PBS. DLS analysis after 24 h showed that only TPP-AIE formed nano-aggregates, with an average size of 610 nm (Fig. 1b). This was further confirmed by transmission electron microscopy (TEM). Nanoparticles were observed in the reaction solution after 24 h incubation (Fig. 1c). These results indicate that the reaction of TPP-Hyd with Ald-Br can occur efficiently, and induces the formation of nano-aggregates that emit green fluorescence.

We observed that the AIE behavior following carbonyl ligation was dependent on the concentration of the reactants (TPP-Hyd and Ald-Br), measured by monitoring fluorescence emission with different concentrations (0.1, 0.2, 0.4, 0.5, 1.0, 2.0 mM) of TPP-Hyd and Ald-Br after 24 h stirring in pH 8.0 PBS. The 0.3 mM mixture emitted bright fluorescence with 365 nm excitation, while fluorescence was not observed in more dilute concentrations (0.1, 0.2 mM) (Fig. 1d and e). This suggested that a critical concentration of reactants was required to induce effective carbonyl ligation. To estimate the critical concentration in the mitochondria mimic solution (pH 8.0 PBS), we analyzed the relationship between the fluorescence and concentration more precisely. We estimated that ~0.41 mM of TPP-Hyd and Ald-Br were required to induce aggregation in mitochondria mimic solution (Fig. 1f). These results indicated that concentrations of TPP-Hyd and Ald-Br greater than 0.41 mM were required to induce AIE by carbonyl ligation in the mitochondrial environment. Furthermore, time-dependent carbonyl ligation was observed in the mixture of 0.5 mM TPP-Hyd and Ald-Br. The fluorescence of TPP-AIE was not observed at initial state, but a bright fluorescence was observed within 3 h (Fig. S3†). It suggested that reaction time more than at least 3 h was also required to form TPP-AIE by carbonyl ligation.

Intra-mitochondrial carbonyl ligation and mitochondrial dysfunction

Triphenylphosphonium (TPP) can drive the accumulation of molecules inside the mitochondria, allowing a critical concentration of bio-orthogonal reactants to accumulate to form nano-aggregates with AIE properties.[27] To investigate the intra-mitochondrial synthetic reaction, we observed fluorescence of TPP-AIE in HeLa cells co-treated with TPP-Hyd and Ald-Br for 3 h. Co-incubation of 20 μM TPP-Hyd and Ald-Br with HeLa cells did not initially show any fluorescence, and weak green fluorescence was observed after incubation for 1 h (Fig. 2a). The intensity of green fluorescence was enhanced with increasing

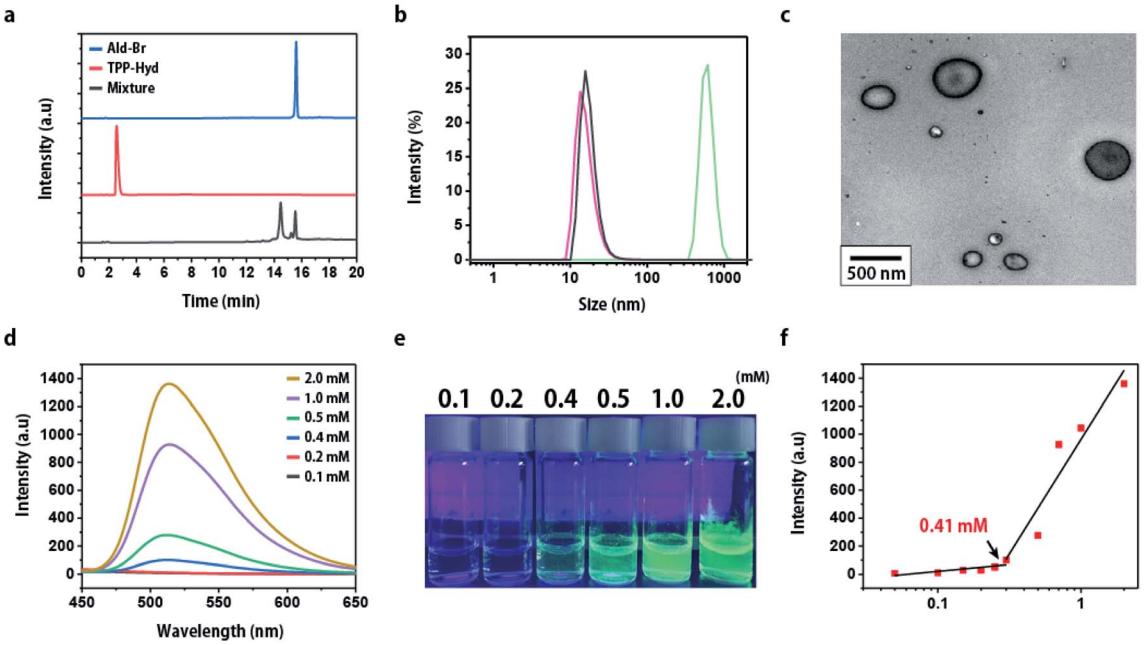

Fig. 1 (a) HPLC trace showing the carbonyl ligation reaction with 1 mM TPP-Hyd and Ald-Br in pH 8.0 PBS. The intensity of the molecules was determined after stirring in mitochondrial mimic solution for 24 h. (b) DLS analysis of TPP-Hyd, Ald-Br, and the mixture of TPP-Hyd and Ald-Br after stirring in pH 8.0 PBS for 24 h. (c) TEM image of TPP-AIE. The mixture of 1 mM TPP-Hyd and Ald-Br was stirred in pH 8.0 PBS for 24 h without further purification. (d) Concentration-dependent fluorescence spectra for the mixture of TPP-Hyd and Ald-Br (0.1, 0.2, 0.3, 0.5, 1.0, and 2.0 mM). (e) Optical image of the mixture for showing appearance of fluorescence with 365 nm irradiation. (f) Quantification of intensity of images in (e) and estimation of the inflection point at which concentrations of TPP-Hyd and Ald-Br induced aggregate formation.

incubation time, and after 3 h incubation, fluorescence intensity was about 2.5 times higher than after 1 h (Fig. 2a and c). Green fluorescence co-localized with red fluorescence of Mitotracker, a mitochondrial marker, as confirmed by Pearson's correlation coefficient (0.927) (Fig. 2b). In contrast, green fluorescence was not observed in HEK293 cells even after 3 h treatment (Fig. S4†). To analyze the effect of carbonyl ligation, the control molecule TPP-Met was co-incubated with Ald-Br in HeLa cells for 3 h. As shown in Fig. S5,† the green fluorescence could not be detected, suggesting that carbonyl ligation can selectively occur inside the mitochondria of cancer cells. The intra-mitochondrial carbonyl ligation was evaluated to estimate

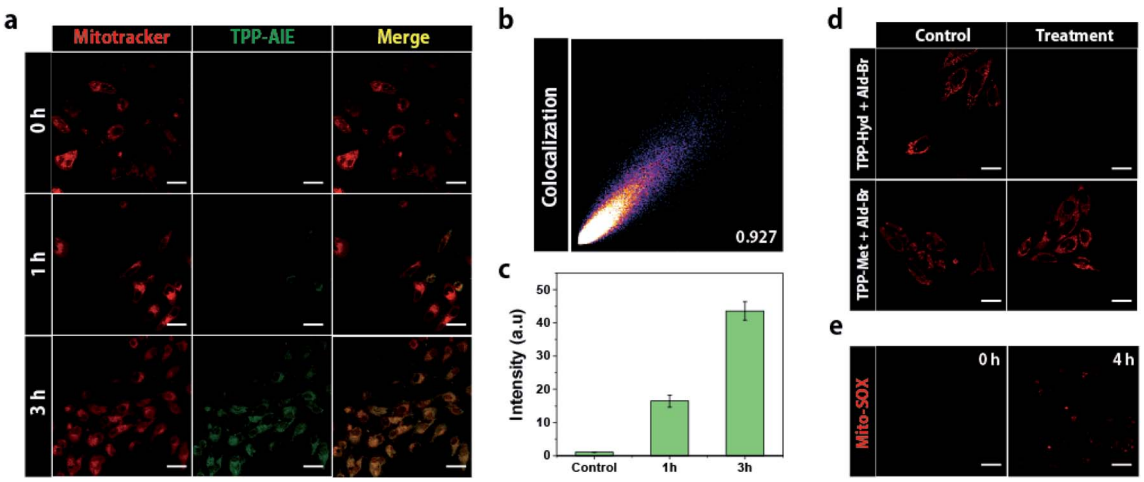

Fig. 2 (a) Confocal laser scanning microscopy (CLSM) images of HeLa cells co-treated with 20 μM TPP-Hyd and Ald-Br for 3 h. The fluorescence of TPP-AIE was observed at 520 nm following 488 nm excitation. (b) Colocalization value between Mitotracker and TPP-AIE. (c) Quantification TPP-AIE in isolated mitochondria from HeLa cells co-incubated with TPP-Hyd and Ald-Br for 1 or 3 h. The intensity was monitored at 520 nm following 488 nm excitation in isolated mitochondria solution. (d) Confocal microscopy images showing mitochondrial membrane depolarization using TMRM in HeLa cells co-incubated with 20 μM TPP-Hyd and Ald-Br for 4 h. (e) CLSM images showing generation of ROS in HeLa cells co-treated with 20 μM TPP-Hyd and Ald-Br for 4 h. Scale bar for all images = 30 μm.

the amount of TPP-AIE inside mitochondria. TPP-Hyd and Ald-Br were incubated with HeLa cells and HEK293 cells, and the fluorescence at 525 nm was monitored in mitochondria-isolated solution. The executed calculation showed that 7 mM and 12 mM TPP-AIE were formed in the cancerous mitochondria when 10 μM and 20 μM TPP-Hyd and Ald-Br were incubated, respectively. Furthermore, the formation level of TPP-AIE in the normal cells was 3 times less than the mitochondria in cancer cells (Fig. S6†).

We expected that intra-mitochondrial carbonyl ligation would exacerbate mitochondrial dysfunction in cancer cells. To address this hypothesis, depolarization of mitochondrial membranes was investigated by using tetramethylrhodamine methyl ester (TMRM), which shows the disappearance of red fluorescence in response to depolarization of the membrane.[28] Red fluorescence was analyzed in both HeLa cells and HEK293 cells co-treated with 20 μM TPP-Hyd and Ald-Br; red fluorescence faded in HeLa cells, while HEK293 cells still emitted red fluorescence after 4 h. In contrast, the red fluorescence remained in the HeLa cells after co-treatment with TPP-Met and Ald-Br (Fig. 2d). This suggested that carbonyl ligation can selectively induce depolarization of mitochondrial membranes in cancer cells.

Mitochondrial damage can contribute to the generation of reactive oxygen species (ROS), which leads to oxidative stress and cell death. The generation of ROS was monitored using Mito-SOX, which emits red fluorescence in response to elevated ROS levels surrounding mitochondria. Red fluorescence was observed in HeLa cells treated with 20 μM TPP-Hyd and Ald-Br for 4 h, while red fluorescence was not observed in HeLa cells co-treated with TPP-Met and Ald-Br (Fig. 2e and S7†). These data revealed that intra-mitochondrial carbonyl ligation can induce oxidative stress and the generation of ROS.

Table 1 IC_{50} against each cell lines

Tissue sources	Cell lines	IC_{50} (μM)
Mouse squamous cell carcinoma	SCC7	25.2
Human breast cancer	MDA-MB-468	22.3
Human cervix cancer	HeLa	15.2
Human breast cancer	SKBR3	25.2
Human breast cancer	MCF7	21.1
Noncancerous fibroblast	HEK293T	52.7
Noncancerous fibroblast	NIH-3T3	56.2

Intra-mitochondrial carbonyl ligation induces cellular apoptosis

As intra-mitochondrial carbonyl ligation selectively induces mitochondrial dysfunction in cancer cells, and mitochondria are associated with cellular death, we hypothesized that intra-mitochondrial carbonyl ligation could induce cellular death specifically in cancer cells. To investigate cellular damage, we first analyzed intracellular ATP levels, an important energy source for maintaining cellular function. This analysis showed

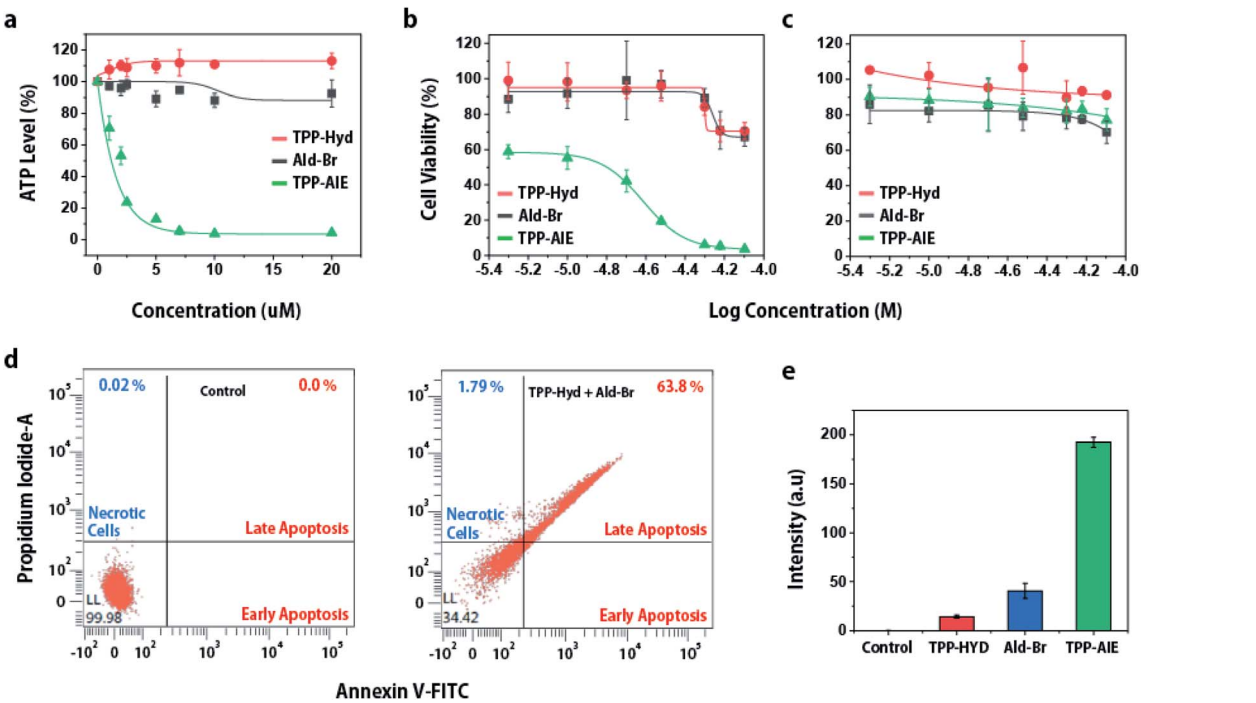

Fig. 3 (a) ATP levels in HeLa cells after treatment for 12 h. Cellular viability of (b) HeLa cells and (c) HEK293 cells treated with different concentrations of TPP-Hyd and Ald-Br. (d) FACS analysis showing annexin V-FITC/PI in cell death. (e) Fluorescence intensity showing activation of caspases-3/7 in HeLa cells co-incubated with 20 μM TPP-Hyd and Ald-Br for 12 h. The activity of caspases-3/7 were monitored by using a fluorescent detection reagent at 530 nm. The signal intensity from TPP-AIE was subtracted from caspase-3/7 detection reagent signal intensity.

that HeLa cells co-treated with TPP-Hyd and Ald-Br exhibited low levels of ATP. Depletion of ATP induces protein denaturation and the destruction of cellular structures, leading to cancer cell death.[29] To investigate anticancer effects, we analyzed cellular viability of cancer cells and normal cells for 48 h. The cytotoxicity was not observed in both cancer cells and normal cells when they were co-incubated with TPP-Hyd and Ald-Br for 12 h (Fig. S8†). However, co-incubation with TPP-Hyd and Ald-Br for more than 24 h showed toxicity in cancer cells with a half-inhibitory concentration (IC_{50}) of 15.2 μM, while toxicity was reduced in normal cells (Fig. 3b and c). In contrast, no toxicity was observed in either HeLa cells or HEK293 cells when incubated with only TPP-Hyd or Ald-Br individually. These results indicate that intra-mitochondrial carbonyl ligation can selectively lead to cellular death in cancer cells. To investigate the mechanism of cell death, we used fluorescence-activated cell sorting (FACS) to investigate fluorescence of annexin V-FITC/PI staining in HeLa cells treated with 20 μM TPP-Hyd and Ald-Br for 12 h. 63.8% of cells lapsed into late-phase apoptosis after co-treatment with TPP-Hyd and Ald-Br compared to untreated cells (Fig. 3d). To verify this mechanism of cell death, we also measured activation of caspases-3/7, which are crucial elements of the apoptotic process, in HeLa cells after 12 h treatment. The activity of caspases-3/7 was analyzed using a detection kit, which emitted green fluorescence in response to caspases-3/7 activation, and calculated signals from TPP-AIE. Caspases-3/7 were significantly activated only in cells co-treated with TPP-Hyd and Ald-Br (Fig. 3e). These results indicate that intra-mitochondrial carbonyl ligation reactions can activate caspase-3/7-dependent apoptosis in cancer cells.

Since mitochondria play an essential role in cellular activity, dysfunction of the mitochondria can lead to apoptosis of cancer cells. The intra-mitochondrial carbonyl ligation induces mitochondrial dysfunction, which is expected to lead to anticancer effects. To investigate this, we analyzed cytotoxicity of intra-mitochondrial carbonyl ligation in various cancer cell lines (SKBR3, MCF7, MDA-MB-468, SCC7) and normal cell lines (NIH3T3, HEK293). This synthetic reaction exhibited toxicity toward cancer cell lines with an IC_{50} of 15–25 μM (Table 1 and Fig. S10†), while it demonstrated lower toxicity toward normal cell lines with an IC_{50} of ~55 μM. Overall, the data indicate that intra-mitochondrial carbonyl ligation can specifically induce cellular death of cancer cells. Thus, these results suggested that intra-mitochondrial carbonyl ligation can have potential application as a therapeutic agent.

Conclusions

In conclusion, we developed an intra-mitochondrial carbonyl ligation reaction that could induce mitochondrial dysfunction to regulate apoptosis of cancer cells. TPP-AIE is generated by bio-orthogonal reactions in which TPP-Hyd reacts with Ald-Br, forming nanoparticles with properties of aggregation-induced fluorescence. As AIE was dependent on the concentration of the reactants, mitochondrial accumulation would promote effective conditions for formation of nano-aggregates. The formed nano-aggregates induce depolarization of mitochondrial membranes and promote oxidative stress, leading to mitochondrial dysfunction. As mitochondria are the primary organelles in cellular energy production, mitochondrial dysfunction induces apoptosis in cancer cells. The anticancer effect was evident in various cancer cell lines. Thus, this novel approach is expected to have potential therapeutic applications as an agent for anticancer treatment.

Conflicts of interest

There are no conflicts to declare.

Acknowledgements

This work was supported by the National Research Foundation of Korea (2017K1A3A1A19071083), and UNIST Basic Science Institute (1.200081.01).

Notes and references

1 L. Dehmelt and P. I. H. Bastiaens, *Nat. Rev. Mol. Cell Biol.*, 2010, **11**, 440–452.
2 S. Soh, M. Byrska, K. K. Grzybowska and B. A. Grzybowski, *Angew. Chem., Int. Ed.*, 2010, **49**, 4170–4198.
3 J. Heo, K. J. Thomas, G. H. Seong and R. M. Crooks, *Anal. Chem.*, 2003, **75**, 22–26.
4 T. J. Piva and E. M. Bowe, *J. Cell. Biochem.*, 1998, **68**, 213–225.
5 G. Liang, H. Ren and J. Rao, *Nat. Chem.*, 2010, **2**, 54–60.
6 D. Ye, A. J. Shuendler, L. Cui, L. Tong, S. S. Tee, G. Tikhomirov, D. W. Felsher and J. Rao, *Nat. Chem.*, 2014, **6**, 519–526.
7 W. Du, Y. Chong, X. Hu, Y. Wang, Y. Zhu, J. Chen, X. Li, Q. Zhang, G. Wang, J. Jiang and G. Liang, *Adv. Funct. Mater.*, 2020, **30**, 1908073–19808086.
8 E. M. Sletten and C. R. Bertozzi, *Angew. Chem., Int. Ed.*, 2009, **48**, 6974–6998.
9 M. King and A. Wagner, *Bioconjugate Chem.*, 2014, **25**, 825–839.
10 D. M. Patterson, L. A. Nazarova and J. A. Prescher, *ACS Chem. Biol.*, 2014, **9**, 592–605.
11 Y. Zeng, T. N. C. Ramya, A. Dirksen, P. E. Dawson and J. C. Paulson, *Nat. Methods*, 2009, **6**, 207–209.
12 J. B. Haun, N. K. Devaraj, S. A. Hilderbrand, H. Lee and R. Weissleder, *Nat. Nanotechnol.*, 2010, **5**, 660–665.
13 S. Ye, S. Wang, D. Gao, K. Li, Q. Liu, B. Feng, L. Qiu and J. Lin, *Bioconjugate Chem.*, 2020, **31**, 174–181.
14 S. Kiran, Z. Hai, Z. Ding, L. Wang, Y. Liu, H. Zhang and G. Liang, *Chem. Commun.*, 2018, **54**, 1853–1856.
15 X. Ai, C. J. H. Ho, J. Aw, A. B. E. Attia, J. Mu, Y. Wang, X. Wang, Y. Wang, X. Liu, H. Chen, M. Gao, X. Chen, E. K. L. Yeow, G. Liu, M. Olivo and B. Xing, *Nat. Commun.*, 2016, **7**, 10432.
16 D. Jagnanan, W. C. Sessa and D. Fulton, *Am. J. Physiol.: Cell Physiol.*, 2005, **289**, 1024–1033.
17 M. T. Jeena, L. Palanikumar, E. M. Go, I. Kim, M. G. Kang, S. Lee, S. Park, H. Choi, C. Kim, S. M. Jin, S. C. Bae,

H. W. Rhee, E. Lee, S. K. Kwak and J. H. Ryu, *Nat. Commun.*, 2017, **8**, 26.

18 Q. Hu, M. Gao, G. Feng and B. Liu, *Angew. Chem., Int. Ed.*, 2014, **53**, 1–6.

19 H. Wang, Z. Feng, Y. Wang, R. Zhou, Z. Yang and B. Xu, *J. Am. Chem. Soc.*, 2016, **138**, 16046–16055.

20 B. Jana, A. P. Thomas, S. Kim, I. S. Lee, H. Choi, S. Jin, S. A. Park, S. K. Min, C. Kim and J. H. Ryu, *Chem.–Eur. J.*, 2020, **26**, 10695–10701.

21 Y. Yamada and H. Harashima, *Adv. Drug Delivery Rev.*, 2008, **60**, 1439–1462.

22 S. Kim, L. Palanikumar, H. Choi, M. T. Jeena, C. Kim and J. H. Ryu, *Chem. Sci.*, 2018, **9**, 2474–2479.

23 M. T. Jeena, K. Jeong, E. M. Go, Y. Cho, S. Lee, S. Jin, S. W. Hwang, J. H. Jang, C. S. Kang, W. Y. Bang, S. K. Kwak, S. Kim and J. H. Ryu, *ACS Nano*, 2019, **13**, 11022–11033.

24 M. T. Jeena, S. Lee, A. K. Barui, S. Jin, Y. Cho, S. W. Hwang, S. Kim and J. H. Ryu, *Chem. Commun.*, 2020, **56**, 6265–6268.

25 Y. Yuan, S. Xu, X. Cheng, X. Cai and B. Liu, *Angew. Chem., Int. Ed.*, 2016, **55**, 6457–6461.

26 X. Ni, X. Zhang, X. Duan, H. L. Zheng, X. S. Xue and D. Ding, *Nano Lett.*, 2019, **19**, 318–330.

27 M. Han, M. R. Vakili, H. S. Abyaneh, O. Molavi, R. Lai and A. Lavasanifar, *Mol. Pharmaceutics*, 2014, **11**, 2640–2649.

28 C. J. Zhang, Q. Hu, G. Feng, R. Zhang, Y. Yuan, X. Lu and B. Liu, *Chem. Sci.*, 2015, **6**, 4580–4586.

29 T. V. Nguyen and O. Bensaude, *Eur. J. Biochem.*, 1994, **220**, 239–246.

